Dynamic Simulation of an Electrostatically Actuated Impact Microactuator

X. Zhao, H. Dankowicz, C.K. Reddy, and A.H. Nayfeh

Department of Engineering Science and Mechanics, MC 0219
Virginia Polytechnic Institute and State University
Blacksburg, Virginia 24061, USA, anayfeh@vt.edu

ABSTRACT

We study the dynamics of an electrostatically driven impact microactuator reported by Mita and associates. The microactuator is modeled as a two-degree-of-freedom rigid multibody system. The impact phenomenon is described by a simple impact law based on Newton's coefficient of restitution. The system dynamics is intensively studied. We investigate the influence of various parameters including excitation frequency and voltage.

Keywords: microactuators, electrostatic, impact, dynamic simulation

1 INTRODUCTION

Precise displacement control and manipulation is required in microscopes, optical devices, nanoscale data storage and micro surgery. Microdevices are ideal for micropositioning due to their small sizes. Microactuators used to produce small displacements would need large actuation forces and a long driving distance. Actuators based on impulsive forces provide a solution to this problem, because impact actuation can generate relatively large motion from small displacement [1]. Recently, impact microactuators have attracted a lot of attention due to ease of fabrication, capability of batch processing, robustness to environment, high accuracy and high power [2]–[5].

Microactuators based on impact can generate linear or rotational motion without mechanical linkages such as ball screws or complicated clamping systems. However, impacts make the dynamical system nonsmooth [6]–[8]. The study of nonsmooth dynamical systems is challenging and one cannot just use traditional dynamical system tools to understand their behaviour. It is important to understand the underlying dynamics in order to design a better microactuator.

In the present work, we explore the dynamics of the impact microactuator reported in [5] through numerical simulation. The nonlinear dynamic model is derived, using a rigid multibody approach[8] and an impact law based on Newton's coefficient of restitution. We examine the influence of the system parameters such as the excitation frequency and the amplitude, on the dynamics of the actuator for specified values of the other system parameters. The objective of the present work is to illustrate the importance of understanding the underlying dynamics in an impact microactuator in order to design a more robust and consistent device.

2 DYNAMIC MODEL

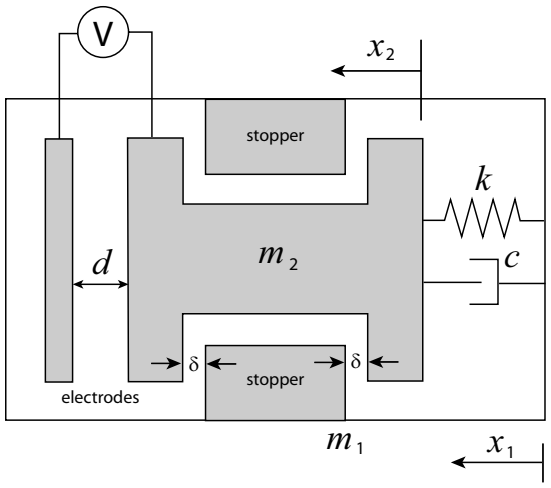

Figure 1: The schematic of the impact microactuator.

A schematic planform of the microactuator is shown in Fig. 1. The system consists of a movable block m_2, which is connected to m_1 by a linear spring with viscous damping. The stoppers and the electrode are rigidly fixed to the frame. The movable mass acts as one of the electrodes. The frame rests on the horizontal ground. Friction between the frame and the ground is assumed to be Coulomb. We denote the coefficient of static friction by μ_s, and that of dynamic friction by μ_d. When a driving voltage, $v(t)$, is applied between the electrodes, m_2 is accelerated towards the stopper till there is an impact. The impact impulse is large enough to overcome the static friction between the frame and the ground. This produces a small displacement of the frame. The minimum stepsize determines the resolution of the microactuator. When a periodically varying voltage is applied, there are repeated impacts and the frame moves by a certain amount during each cycle, thereby producing the needed displacement over a period of time. The

equations of motion of the system can be written as

$$m_1\ddot{x}_1 = F \tag{1}$$

$$m_2(\ddot{x}_1 + \ddot{x}_2) + kx_2 + c\dot{x}_2 = \frac{\alpha v(t)^2}{(d-x_2)^2} \tag{2}$$

where x_2 is the displacement of m_2 relative to m_1, and x_1 is the displacement of m_1 relative to the ground. We note that $\alpha = \frac{1}{2}\epsilon_0 A$, where ϵ_0 is the permittivity of free space, A is the overlap area, and d is the zero-voltage gap between the electrodes. As m_1 moves, the total force on m_1, F is

$$F = kx_2 + c\dot{x}_2 - \frac{\alpha v(t)^2}{(d-x_2)^2} - \mu_d N \text{ sign}(\dot{x}_1) \tag{3}$$

where N is the normal reaction. We assume that gravity is the only external force, in which case $N = (m_1+m_2)g$. When m_1 is stationary,

$$F = 0 \text{ and } |kx_2 + c\dot{x}_2 - \frac{\alpha v(t)^2}{(d-x_2)^2}| \leq \mu_s N \tag{4}$$

As shown in Fig. 1, the separation between m_2 and the stoppers is δ. When $|x_2| = \delta$, m_2 impacts with the stopper. Let v_1 and v_2 be the velocities of m_1 and m_2 respectively, just before impact, and v_1' and v_2' be the velocities after impact. Assuming that the collision between m_1 and m_2 is inelastic with a restitution coefficient e, conservation of linear momentum yields [9]

$$v_1' = v_1 + \frac{(1+e)m_2}{m_1+m_2}v_2 \tag{5}$$

$$v_2' = -ev_2 \tag{6}$$

3 NUMERICAL SIMULATION

The equations of motion derived in the previous section are piecewise smooth due to impacts and friction. The dynamics can be divided into two different phases. In the first phase only m_2 is in motion, described by Eqs. (1), (2), and (4). In the second phase both m_1 and m_2 are in motion, described by Eqs. (1)-(3). The integration procedure is shown in Fig. 2, where impact map is described by Eqs. (5) and (6).

Direct numerical integration generates results qualitatively consistent with those reported in [5]. A sinusoidal voltage of 100V at 1HZ is applied in the experiments [10] and the average displacement is found to be 20nm/impact. Parameter values reported by Mita et al. are used for the numerical simulation. The parameter values not reported are fitted to obtain a displacement per impact of approximately 20 nm. Figure 3 shows the relationship between the displacement and voltage. We note that there are two impacts in one excitation cycle, consistent with the experimental observations.

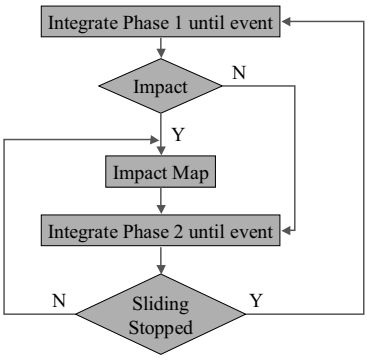

Figure 2: Flowchart of the algorithm.

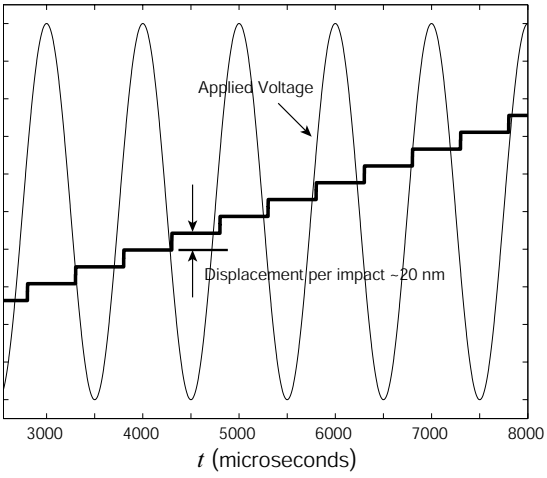

Figure 3: Displacement per impact.

4 SWITCH ON AND OFF MECHANISM

In this paper, we apply a sinusoidal voltage of the form $v(t) = f\cos(\omega t)$. We treat the amplitude f and frequency ω as our design variables and study the dynamics with respect to them. The system parameter values used for simulations are $m_1 = 5$, $m_2 = 1$, $k = 1$, $c = 0.04$, $d = 1$, $\delta = 0.5$, $e = 0.8$, $\mu_s = 0.4$, $\mu_d = 0.27$, and $\alpha = 1$.

The system possesses two types of steady orbits: those with impacts and those without impacts. In a previous paper [9], we have investigated the bifurcation of the impact orbits. One interesting question is how the system transfers back and forth between impact and non-impact orbits when changing parameters. In this paper, we call the impact orbits "on" status, and the non-impact orbits "off" status. Therefore the switch on and off mechanism is the interest of this study. Three different types of switch on and off mechanism are found for the microactuator.

To visualize the switch on and off scheme, a Poincaré

section [11] is chosen at $x_2 = 0$ in the state space. One example of type I switch on and off mechanism is shown in Fig. 4 for $\omega = 0.5$. Figure 4 shows the variation of v_2 on the Poincaré section with respect to the applied voltage f. When $f = 0.16$, the voltage is not strong enough to drive the microactuator. Here, the frame is held still by static friction, and the amplitude of the movable block is less than δ. As the voltage is slowly increased, the maximum displacement of m_2 approaches δ. At a critical voltage, a grazing periodic solution is established as zero-velocity contact occurs between the movable block and the stopper. As seen in the diagram, a further increase in f results in a transition of the asymptotic dynamics to an impacting solution with relatively large impact velocity. On the other hand, when $f = 0.24$ the system exhibits a periodic orbit with one impact per period, which is called period one impact orbit. Reducing the voltage decreases the impact velocity and therefore the step movement of the microactuator. When a critical voltage is reached, an eigenvalue of the Jacobian of the Poincaré map corresponding to the impacting solution equals 1. This corresponds to a cyclic fold bifurcation and no impacting solution exists if the voltage is reduced further. Instead, a further reduction in f results in a transition of the asymptotic dynamics to a non-impacting solution with relatively small amplitude. Figure 4 shows the presence of hysteresis when the system is switched on and off.

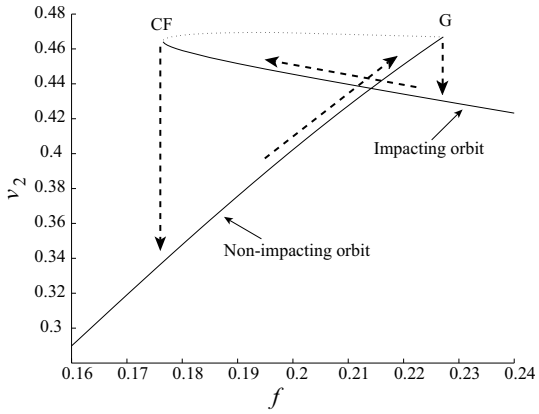

Figure 4: Type I switch on and off mechanism. G indicates a grazing bifurcation and CF a cyclic fold bifurcation.

Figure 5 shows the type II switch on and off mechanism for $\omega = 0.485$. When $f = 0.171$, m_1 is held still by static friction, and m_2 is oscillating with an amplitude smaller than δ. As the voltage is slowly increased, the amplitude of m_2 increases. When a critical voltage is reached, grazing impact occurs. A narrow impact chaotic band immediately follows the grazing when the voltage is increased slightly. On the other hand when $f = 0.177$, the system exhibits a period one impact orbit. When the voltage is slowly decreased, the system exhibits a period doubling route to chaos. When the voltage is further decreased, the chaotic band touches the non-impact periodic orbit at grazing. Type II does not show hysteresis.

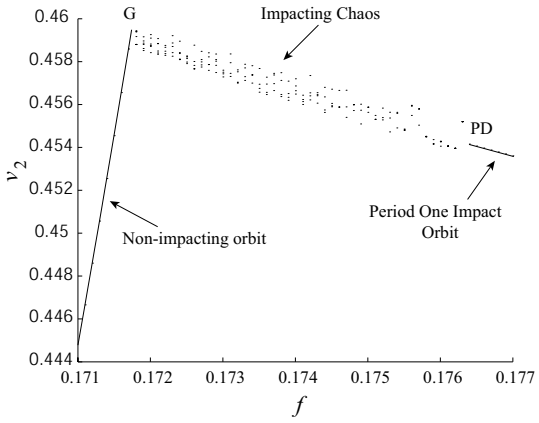

Figure 5: Type II switch on and off mechanism. G indicates a grazing bifurcation and PD a period-doubling bifurcation.

An example of type III switch on and off mechanism is shown in Fig. 6, for $\omega = 0.45$. At low voltages, the microactuator is "off". As the voltage is slowly increased, the oscillation amplitude of m_2 increases. Before the amplitude of m_2 is large enough to touch the stopper, there is a cyclic fold bifurcation at the critical voltage $f = 0.2356$. Slightly increasing the voltage beyond the critical value causes the system jump to a chaotic impact orbit. When the voltage is decreased, the chaotic impact orbit persists until it touches an unstable non-impact orbit at $f = 0.2355$. On the other hand, when $f = 0.29$, the system exhibits a period one impact orbit. When the voltage is slowly decreased, the system becomes chaotic through a period doubling sequence.

The different behavior regimes are shown in the $f-\omega$ parameter space in Fig. 7. The solid line denoted the switch on boundary and the dotted line denoted the switch off boundary. When $\omega > 0.489$, the switch on and off mechanism is type I. When $0.480 < \omega < 0.489$, the system undergoes type II switch on and off mechanism. Type III mechanism is experienced when $\omega < 0.480$. A chaotic band follows the switch on voltage in both type II and type III. Both type I and type III have hysteresis. To produce accurate and predictable displacement, it is necessary to operate the microactuator in a periodic manner with impact occuring once each period. Because the existence of chaos in type II and type III, excitation frequencies in the type I range is favorable.

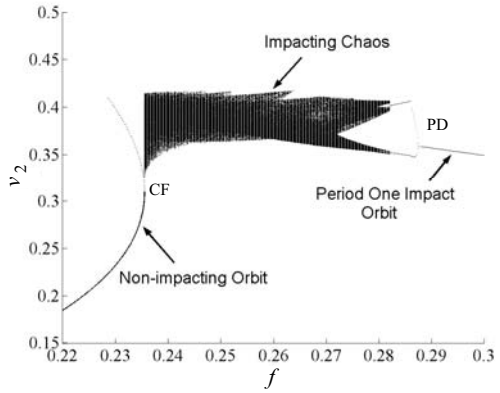

Figure 6: Type III switch on and off mechanism. CF indicates a cyclic fold bifurcation and PD a period-doubling bifurcation.

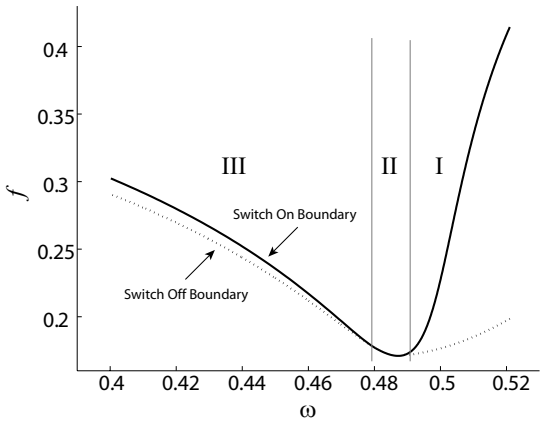

Figure 7: Variation of switch on and off voltages with respect to the excitation frequency.

5 CONCLUSIONS

Micro impact actuators are suitable for high resolution with large travel range. We have studied the dynamics of an impact microactuator modeled as a system of two coupled rigid bodies. A periodically varying excitation voltage is applied. Impacts make the vector field discontinuous and render the system nonsmooth. The numerical simulations presented above clearly show the complex dynamics exhibited by the simple model. The influence of the excitation frequency and amplitude on the dynamic behavior is examined. The numerically obtained displacement/impact values are consistent with the experiment. The numerical results bring out the importance of understanding the underlying dynamics so as to ensure a robust and consistent device operation.

REFERENCES

[1] Ragulsikis, K., Bansevicus, Barausleas, R., and Kulvietis, G., *Vibromotors for Precision Microrobots*, New York: Hemisphere, pp. 289-295, 1988.

[2] Lee, A.P., Nikkel, D.J. Jr., and Pisano, A.P., "Polysilicon Linear Microvibromotors", in *Proc. 7th Int. Conf. Solid-State Sensors and Actuators*, Vol. 1(2), pp. 46-49, 1993.

[3] Daneman, M.J., Tien, N.C., Solgaard, O., Pisano, A.P., Lau, K.Y., and Muller, R.S., "Linear Microvibromotor for Positioning Optical Components", *IEEE Journal of Microelectromechanical Systems*, Vol. 5(3), pp. 159-165, 1996.

[4] Saitou, K., Wang, D.A., and Wou, S.J., "Externally Resonated Linear Microvibromotor for Microassembly", *IEEE Journal of Microelectromechanical Systems*, Vol. 9(3), pp.336-346, 2000.

[5] Mita, M., Arai, M., Tensaka, S., Kobayashi, D., and Fujita, H., "A micromachined impact microactuator driven by electrostatic force", *IEEE Journal of Microelectromechanical Systems*, Vol. 12(1), pp. 37-41, 2003.

[6] Shaw, S. W., and Holmes, P. J., A periodically forced piecewise linear oscillator, *Journal of Sound and Vibration*, Vol. 90(1), pp. 129-155, 1983.

[7] Nordmark, A.B., *Grazing Conditions and Chaso in Impacting Systems*, Ph.D. Thesis, Royal Institute of Technology Stockholm, Sweden, 1992

[8] Brogliato, B., *Nonsmooth Mechanics*, Springer-Verlag, New York, 1999.

[9] Zhao, X., Reddy, C.K., Nayfeh, A.H., "Bifurcations and Chaotic Dynamics in an electrostatically Actuated Impact Microactuator: a Numerical Exploration", *ASME International 19th Biennial Conference on Mechanical Vibration and Noise*, DETC2003/VIB-48519, Chicago, Illinois, 2003.

[10] Personal communication with Dr. Makoto Mita.

[11] Nayfeh, A. H., and Balachandran, B., *Applied Nonlinear Dynamics: Analytical, Computational, and Experimental Methods*, Wiley, New York, 1995.